Cellular and Molecular Neurobiology (2019) 39:1081–1092
https://doi.org/10.1007/s10571-019-00703-6

ORIGINAL RESEARCH

Lidocaine Potentiates SOCS3 to Attenuate Inflammation in Microglia and Suppress Neuropathic Pain

Yan Zheng[1] · Xuhui Hou[2] · Songbai Yang[2]

Received: 13 November 2018 / Accepted: 8 June 2019 / Published online: 17 June 2019

Abstract

Lidocaine is one of the typical local anesthetics that are frequently used in the peripheral nerve blocks and pain management. Emerging evidence have shown that lidocaine may exert anti-inflammatory effect involving neuropathic pain. However, the effect and underlying mechanism of lidocaine in suppressing neuroinflammation in neuropathic pain are incompletely revealed. In this study, effects of lidocaine on the suppressors of cytokine-signaling protein 3 (SOCS3) in microglia are investigated in chronic constriction injury (CCI) rat model and lipopolysaccharide (LPS)-stimulated BV-2 cells. It was shown that intrathecal injection of lidocaine substantially alleviated CCI-induced neuropathic pain, as reflected by the decreased thermal latency and mechanical threshold. Lidocaine reduced the CCI-evoked spinal injury and cell apoptosis. CCI induced an significant increase of IBA1$^+$ microglia accompanied by the increase of inflammatory cytokines IL-6 and IL-1β, which were suppressed after lidocaine administration. SOCS3 expression in IBA1$^+$ microglia was notably upregulated in response to lidocaine injection, which presented in a similar pattern in LPS-activated BV-2 cells. Furthermore, lidocaine upregulated SOCS3 expression dependent of pCREB, and CREB silencing greatly discounted this effect. The intrathecal injection of lentiviral vectors LV-SOCS3 efficiently alleviated CCI-evoked neuropathic pain and reduced spinal IBA1$^+$ microglia. SOCS3 overexpression contributed to the inhibition of neuroinflammation by decreasing the expression and activation of p38 MAPK and NF-κB stimulated by LPS. Collectively, lidocaine promoted the SOCS3 expression in microglia, in turn leading to suppression of IBA1$^+$ microglia accumulation and p38 MAPK and NF-κB, which may expand our understanding on lidocaine in suppressing neuroinflammation and neuropathic pain.

Keywords Lidocaine · Microglia · Neuropathic pain · SOCS3 · Neuroinflammation

Introduction

Peripheral nerve injury can result from various diseases or surgeries (e.g., limb or colon amputation, thoracotomy). It often results in abnormal chronic pain and pain hypersensitivity, known as neuropathic pain (Kwon et al. 2017). Peripheral sensory nerve fibers, which extend from cell bodies in the dorsal root ganglion, capture mammalian nociceptive inputs. These inputs are conducted by action potentials in primary afferent fibers to the second-order neurons in the spinal dorsal horn and then the nociceptive cortex (Cohen and Mao 2014; Jensen and Finnerup 2014). Neuropathic pain always has adverse impacts on quality of life of the patient. It creates high economic burden on the individual and society. Despite improvement in the etiology and management of pain, many patients do not have complete solutions for their neuropathic pain in clinical practice (Finnerup et al. 2015; Gierthmuhlen and Baron 2016).

Local anesthetics (e.g., lidocaine, ropivacaine, bupivacaine) reversibly block voltage-gated sodium channels to reduce the excitability of neurons. They are frequently used for peripheral nerve blocks, epidural and spinal anesthesia, and pain management. Their use is associated with a low prevalence of severe side effects (Becker and Reed 2012; Eberhardt et al. 2017; Leffler et al. 2011). In addition to the effect of blocking action potential propagation, local

Yan Zheng and Xuhui Hou contributed equally to this work.

✉ Songbai Yang
songbaiyangres@163.com

[1] Department of Anesthesiology, China-Japan Union Hospital, Jilin University, Changchun 130033, Jilin, China

[2] Department of Vascular Surgery, China-Japan Union Hospital, Jilin University, No. 126 Sendai Street, Changchun 130033, Jilin, China

anesthetics have anti-inflammatory effect, such as inhibition of phagocytosis in macrophages or leucocytes and suppression of the adhesion of granulocytes (Gray et al. 2016; Kuchalik et al. 2017).

Microglial cells are prominent glial cells in the spinal cord that contribute to the sensitization and maintenance of chronic pain. Cortical and spinal microglia are important immunological components of the central nervous system (CNS) that play crucial roles in regulating inflammatory responses in various CNS disorders (Matsuura et al. 2012). Activated microglia proliferate, migrate, change shape, and perform phagocytosis. They also secrete biologically active substances and inflammatory mediators that contribute to neuropathic pain by activating nociceptive neurons (Berta et al. 2017; Costigan et al. 2009). Lidocaine pretreatment can suppress gene expressions of proinflammatory cytokines in microglia after nerve injury (Yuan et al. 2014). However, the underlying mechanisms remain unclear.

The suppressors of cytokine signaling (SOCS) protein family comprises eight members (SOCS1–SOCS7 and CIS). These proteins control cytokine signaling to eliminate severe and systemic inflammation (Yin et al. 2015). SOCS3 dysregulation occurs in many autoimmune diseases, including systemic lupus erythematosus, rheumatoid arthritis, type 1 diabetes, and multiple sclerosis (Liang et al. 2014). *SOCS3* gene silencing increases the proliferative and inflammatory responses in macrophages (Ohno-Urabe et al. 2018). Recent findings also demonstrate that SOCS3 upregulation attenuates postoperative pain (Fan et al. 2018; Wei et al. 2017). However, whether SOCS3 is involved in lidocaine-suppressed neuropathic pain is unknown. Therefore, our study aims to investigate whether lidocaine can modulate SOCS3 expression and activity to inhibit spinal microglia activation and to investigate the underlying mechanisms of SOCS3 in suppressing neuroinflammation.

Materials and Methods

Experimental Animals and Neuropathic Pain Model

Adult male Sprague–Dawley rats (8–10 weeks old, weighing 250–280 g) were obtained from the animal center of Jilin University, and kept in an animal care facility with mild temperature, mild humidity, a 12-h dark/light cycle, and free access to fresh food and water. All experimental procedures were approved by the Institutional Animal Care and Use Committee of Jilin University and complied with the Guidelines for the Care and Use of Laboratory Animals. We made every effort to limit the number of animals used and to minimize suffering of the animals.

The animals were randomly divided into four groups: sham + saline, sham + lidocaine (Lido), CCI + saline, and CCI + Lido ($n = 12$ for each group). Rats in the two CCI groups underwent surgery to cause chronic constriction injury (CCI) for inducing neuropathic pain, as previously described (Toda et al. 2011). In brief, all rats were exposed to isoflurane anesthesia before blunt dissection surgery to expose the left (ipsilateral) common sciatic nerve at the mid-thigh level. Then, four 4-0 silk threads were loosely tied around the sciatic nerve at intervals of about 1 mm, and the incision area was closed with a 4-0 silk suture. The contralateral sciatic nerve was not touched. For rats in the sham surgery groups, the left sciatic nerve was exposed without silk ligation before tissue sampling.

Catheter Implantation and Drug Administration

On the third day after surgery, intrathecal catheter implantation was performed, as previously described (Zhuang et al. 2006). In brief, following anesthesia by intraperitoneal injection of 10% chloral hydrate, a PE-10 silastic tube was introduced and advanced 2 cm to 3 cm into the intrathecal space and around the lumbar enlargement of the rat spinal cord, ending between L4 and L5. The correct catheter position was confirmed by careful aspiration of cerebrospinal fluid. After catheter implantation, all rats were allowed to recover for 24 h. Rats exhibiting any motor or sensory dysfunction were excluded at 3 days after catheter implantation.

On the 6th day after surgery, rats in sham + Lido and CCI + Lido groups received lidocaine (Sigma, St. Louis, MO, USA) at a concentration of 1.0% that dissolved in 0.9% saline, and rats in sham + saline and CCI + saline groups receiving equal volume of 0.9% saline. All the animals received a constant dose of lidocaine solution (50 μL, 0.5 mg total) or saline (50 μL) within 1 min, respectively, via the implanted catheter. The animals were kept under the same conditions throughout the study.

Animal Behavioral Tests

Mechanic paw-withdrawal latency after stimulation was determined using an electrical von Frey filament (IITC Life Science Inc, Woodland Hill, CA, USA) (Li et al. 2015). In brief, before the series tests, individual rat was placed on an elevated metal grid (5 × 5 mm) covered with a clear plastic cage (20 × 25 × 15 cm) and allowed to acclimate to the test conditions for approximately 30 min. The von Frey filament was fixed to the handheld pressure transducer, and a thin probe was applied perpendicularly to the medial surface of the rat' s hind paw with gradually increasing force. The test was automatically terminated when the animal withdrew or licked its hind paw, and the latency time was recorded as the paw withdrawal threshold. Stimulations were repeated three times for each rat at 10-min intervals, and the average

paw-withdrawal threshold from three readings was calculated at each time point.

Thermal hyperalgesia was assessed using a Hot Sting instrument (Beijing Zhishuduobao Biological Technology Co. Ltd., Beijing, China), as previously described (Wang et al. 2016). Rats were placed individually on a vitreous test box and allowed to habituate for 30 min. Then, radiant heat was directed to the plantar medial surface of each hind paw, and lifting or licking of the hind paw was considered the endpoint of the test. The thermal withdrawal latency was defined as the time from the onset of radiant heat to the time of hind paw withdrawal, which was shown digitally on a display screen. Before the test schedule, the heat intensity was adjusted to produce a thermal withdrawal latency of 12 s to 15 s in the normal rat. To avoid tissue damage, we set an automatic 30-s latency cutoff. The thermal withdrawal latency in each rat was measured independently three times at 10-min intervals between trials. All experimental rats underwent thermal and mechanical pain tests 3 days before surgery (baseline) and 1 day, 4 days, 7 days, 10 and 14 days post-operatively.

Microglia Cell Culture

Primary murine microglia BV-2 cells were obtained from Sciencell (Carlsbad, CA, USA) and maintained in Dulbecco's Modified Eagle's medium (DMEM, Hyclone/Thermo, Rockford, IL, USA) containing 10% fetal bovine serum (Hyclone/Thermo), penicillin, and streptomycin in 5% CO_2 at 37 °C. The cells were pretreated with 10 μg/mL lidocaine solution or saline for 1 h and then exposed to lipopolysaccharide (LPS) stimulation (1 μg/mL; Sigma-Aldrich, St. Louis, MO, USA) for 24 h.

Histological Analysis of Spinal Cord Injury

At 6 h after the last behavioral test, six animals from each of the four groups were sacrificed for spinal cord histopathologic examination or immunological staining. Rats were killed with chloral hydrate, and the hearts were perfused with 0.9% saline followed by 4% paraformaldehyde. Both anterior and posterior roots in the L4 and/or L5 lumbar segments were dissected by laminectomy, and the samples were preserved in 4% paraformaldehyde at 4 °C. Spinal cords were embedded in OCT and then cut into 14-μm slices in thickness (Leica CM1900, Germany). In the histopathologic and immunological study, ipsilateral spinal dorsal horn of the CCI or sham rats were identified as the focused area of interest. Five sections from L4 and/or L5 lumbar segments of each rat were analyzed.

A commercial TUNEL kit (Biyotime, Shanghai, China) was used to detect apoptotic cells in lidocaine-treated CCI rats or rats that had sham surgeries according to manufacturer instructions. In brief, tissue slides were incubated with 20 μg/mL proteinase K for 15 min at room temperature, and then quenched in 3% hydrogen peroxide for 5 min. After washing in PBS (pH 7.4), specimens were incubated in 1 × equilibration buffer for 10 min. Slides were next incubated with terminal deoxynucleotidyl transferase (Tdt) for 1 h at 37 °C before blocking with stop buffer, and then incubated with peroxidase-conjugated anti-digoxigenin antibody for 30 min at room temperature. The specimens were reacted with diaminobenzidine (DAB; Sigma, St Louis, MO) and counterstained with methyl green. The ratio of the apoptotic cells was calculated using Image-Pro Plus 6.0 (Media Cybernetics, Silver, Spring, USA). Five fields on each section (five sections per rat) were randomly selected and mean percentage of TUNEL positive cells in spinal dorsal horn area in each group ($n = 6$ rats) was calculated and compared.

Immunological Staining

Microglia presentation in response to CCI and post-CCI lidocaine treatment was evaluated using immunohistochemistry staining. Sections from each group (six rats per group) were incubated with IBA1 (1:200, Cell Signaling, Beverly, MA, USA) primary antibody overnight and then were washed with PBS and incubated with the secondary antibody (1:300) for 2 h at room temperature. After being washed three times with PBS, the DAB-stained specimens were observed using an Olympus B × 40 microscope. At least five randomly distributed 40 × fields within the dorsal horn of the spinal cord were captured for each section. The ratios of anti-IBA1 immunoreactivities in the spinal dorsal horn were quantitatively measured using Image-Pro Plus software (Media Cybernetics, MD, USA) and expressed as a percentage of the total area examined.

Double immunofluorescence staining was performed to determine the colocalization of SOCS3 -expressing cells with $IBA1^+$ microglia in response to CCI exposure and lidocaine treatment. For this double labeling, sections were incubated with a mixture of IBA1 (1:200, Cell Signaling, Beverly, MA, USA) or SOCS3 (1:100; Serotec, Indianapolis, IN, USA) primary antibodies for 48 h at 4 °C. Cy3-conjugated or Alexa Fluor 488-conjugated secondary antibodies were used, as appropriate, to visualize the bound primary antibodies. The stained specimens were observed using a fluorescence microscope and recorded using a CCD spot camera. $SOCS3^+$ cells and $IBA1^+$ microglia quantification were performed by counting the cells in five randomly sampled images captured from each spinal cord using an epifluorescence microscope under × 10 objective in Imaging J analysis software (National Institutes of Health, Bethesda, MD,USA).

Reverse Transcription Polymerase Chain Reaction

Total RNA was extracted using TRIZOL reagents (Invitrogen, Carlsbad, CA, USA) from the spinal cords of 6 rats in all 4 groups 6 h after the termination of the behavioral tests or from the treated BV-2 cells after 48 h of incubation. Purity of total isolated RNA was detected using electrophoresis on 1% agarose gel. First-strand cDNA was synthesized using 1 μg of total RNA in a SuperScript® III Reverse Transcriptase system (Invitrogen). PCR amplification was performed using a PCR amplification kit (Takara Biotechnology, Dalian, China). The specific primers were synthesized by Sangon Biotech (Shanghai, China) with the following sequences: for SOCS3, 5′-GCT CCA AAA GCG AGT ACC AGC-3′ (forward) and 5′- AGT AGA ATC CGC TCT CCT GCA G-3′ (reverse); for IL-6, 5′-CCA GAA ACC GCT ATG AAG TTC C-3′ (forward) and 5′-GTT GGG AGT GGT ATC CTC TGT GA-3′ (reverse); and for IL-1β, 5′- TAC AGG CTC CGA GAT GAA CAA C-3′ (forward) and 5′- TTT GAG GCC CAA GGC CAC AG-3′ (reverse). GAPDH was used as an internal control (forward 5′- ACC ACA GTC CAT GCC ATC AC-3′ and reverse 5′- TCC ACC ACC CTG TTG CTG TA-3′). The reaction was performed in an ABI7500 Real-time PCR system (Applied Biosystems, Foster City, CA, USA) with a cycle program as follows: denaturing for 5 min at 95 °C, 40 cycles of 10 s at 95 °C, and 1 min at 60 °C. Relative quantification was calculated and normalized using the $2^{-\Delta\Delta CT}$ method.

Western Blot

Total protein was extracted from treated microglia using the Cell Total Protein Extraction Kit (Amresco, Cleveland, Ohio, USA). The proteins were separated by 12% sodium dodecyl sulfate polyacrylamide gel electrophoresis (SDS-PAGE) followed by electrotransfer to a polyvinylidene difluoride membrane. After blocking nonspecific binding with 5% milk in TBST for 1 h at room temperature, the membranes were probed using primary antibodies against SOCS3 (1:1000), IBA1 (1:1000) (Cell Signaling, Danvers, MA, USA), and cAMP response element binding-protein (CREB)/p-CREB (S133, 1:1000), as well as p-p65(Ser536)/p65 and p-p38(Tyr182)/p-38-MAPK (Abcam, Cambridge, UK) overnight at 4 °C. Then the membranes were labeled with horseradish-peroxidase-conjugated secondary antibodies (1:2000) (Abcam). Bands were revealed with an enhanced chemiluminescence reagent (Millipore, Boston, MA, USA) and recorded on X-ray films. Densitometry of each band was quantified using a Gel Imaging System and Quantity One 4.62 software (Bio-Rad, Hercules, CA, USA).

ELISA

For the evaluation of inflammatory cytokines in the BV-2 cell supernatant, the IL-1β, IL-6 and TNF-α concentrations were evaluated at 24 h after treatment using commercially available ELISA kits (Jiancheng Ltd., Nanjing, China) based on the manufacturer's protocol.

SOCS3-Overexpressing Vector or CREB siRNA Transfections

The lentiviral vectors LV-SOCS3 and LV-Control were purchased from Obio Technology Corp., Ltd. (Shanghai, China). The transfection titer of LV-SOCS3 was 7.5×10^9 PFU/mL. At 3 days before the CCI surgery, 10 μL of LV-SOCS3 or LV-Control was intrathecally injected into the rats ($n = 6$ for each group).To perform intrathecal injections, the rats were placed in a prone position and the midpoint between the tips of the iliac crest was located. A Hamilton syringe with a 30-gauge needle was inserted into the subarachnoid space of the spinal cord between the L4 and L5 spinous processes at a distance 1-mm rostral and caudal to the center of the spinal cord. Proper intrathecal injection was systemically confirmed by observation of a tail flick.

For the transfection of microglia cells with LV-SOCS3 and LV-Ctrl, BV2 were plated in 96-well plates at a density of 2×10^5 cells/well and cultured in DMEM medium for 24 h. Viral particles at a multiplicity of infection (MOI) of 10 and polybrene (8 μg/ml) were added to the wells. After 12 h, the PBS-washed cells were cultured until confluent. Afterwards, cells were dislodged by gentle pipetting and transferred into polyornithine-coated 25 cm^2 culture flasks for expansion.

CREB1 and the matched negative control (NC) siRNA sequences were synthesized by GenePharma (Shanghai, China). The siRNA transfection was performed using Lipofectamine 2000 transfection reagent (Invitrogen, CA, USA). In brief, BV-2 cells were plated in 12-well plates and transfected with the mixture of NC or CREB siRNA (1.0 μg/well) with RNAi Max reagent in serum-free medium. After 4 h, 20% FBS with the transfection media at a volume of 1:1 were added. The cells were incubated for 24 h at 37 °C followed by centrifugation and resuspension for further examinations. The siRNA sequences were as followings: CREB1 siRNA, sense 5′-GGU GGA AAA UGG ACU GGC Utt-3′, antisense 5′-AGC CAG UCC AUU UUC CAC Ctt-3′; NC siRNA, sense 5′-UUC UCC GAA CGU GUC ACG Utt-3′, antisense 5′-ACG UGA CAC GUU CGG AGA Att-3′.

Statistical Analysis

Data are presented as mean ± SD and were analyzed by SPSS19.0 software (IBM, Chicago, IL, USA). Differences

among multiple groups were compared using ANOVA followed by least-significant-difference (LSD) multiple comparison tests. Repeated measures of ANOVA were performed to analyze differences among the behavioral results for the time course across groups. Differences were considered significant at $p < 0.05$.

Results

Lidocaine Suppressed Mechanical and Thermal Pain Induced by Chronic Constriction Injury

We first observed the effect of lidocaine on the behavioral performance of rats that underwent either CCI or sham surgeries. Repeated ANOVA analyses showed that there were significant differences in mechanical withdrawal thresholds among the four groups for the time course ($F = 7.156$, $p = 0.002$), suggesting that CCI injury and/or lidocaine treatment affected mechanical withdrawal thresholds of the tested animals. Intrathecal injection of either saline or lidocaine did not obviously change paw-withdrawal threshold of sham rats within 14 days after the operation. While, the mechanical withdrawal threshold significantly decreased in CCI + saline group as early as 1 day after the injury in comparison with the baseline threshold, and this decrease was maintained until the termination of the behavioral test. Besides, comparing with the CCI + saline group, an intrathecal injection of lidocaine in CCI rats immediately displayed analgesic effect as reflected by the gradually increased mechanical withdrawal thresholds after the injections(Fig. 1a). We also tested the thermal withdraw latency across the four groups and found that lidocaine treatment effectively attenuated CCI-induced pain by decreasing the thermal withdraw latency (Fig. 1b).

At 6 h after the last behavioral tests, six randomly selected rats from each group were sacrificed for histological analysis and TUNEL staining was performed to detect

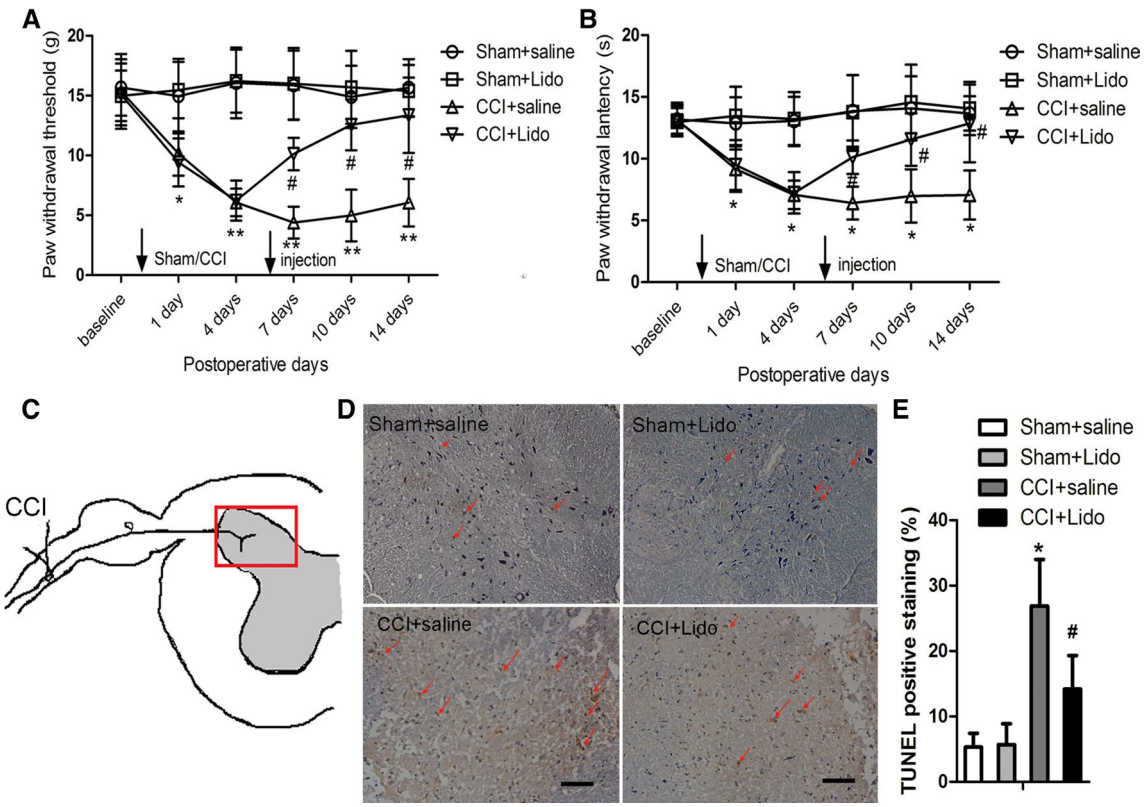

Fig. 1 Effect of intrathecal lidocaine administration on behavioral performance and spinal injury in CCI rats. CCI and sham-operated rats were used to evaluate effects of lidocaine administration on neuropathic pain. Behavioral tests were performed 3 days before CCI as baseline, and 1, 4, 7, 10 and 14 days after CCI. Lidocaine and saline were intrathecally injected into CCI or sham rats 6 days postsurgeries. Histological examinations were performed 6 h after the last behavioral test. Changes of mechanical allodynia (**a**) and thermal hyperalgesia (**b**) in sham and CCI rats at indicated time points in response to Lidocaine injection or not. The differences between groups were analyzed by repeated measures ANOVA followed by LSD tests. $^{**}p < 0.01$, $^{*}p < 0.05$ versus Sham + saline; $^{\#}p < 0.05$ versus CCI + saline. $N = 12$ rats/group; **c** Diagram of the target areas of interest (rectangle box) for histological and immunological studies; **d** TUNEL staining of the spinal dorsal horn in each group of rats; Scale bar: 100 μm **e** Quantification of the ratio of TUNEL stained areas in each group of animals. $N = 6$ rats/group

the early apoptotic cells affected by CCI and/or lidocaine treatment. We then determined the percentage of TUNEL stained cells in the ipsilateral spinal dorsal horn of each animal as depicted in Fig. 1c, and the results showed that 5.31 ± 2.07% TUNEL-stained cells presented in this area of sham-operated rats receiving saline, which were comparable to the ratio in sham rats receiving lidocaine, indicating no neurotoxic effect of lidocaine at the current dose. However, the apoptotic cells increased to 26.90 ± 6.89% in rats that underwent CCI surgery and received saline ($p < 0.05$). Lidocaine injection notably alleviated CCI evoked spinal injury and the apoptotic cell ratio reduced to 14.26 ± 5.13% ($p < 0.05$) (Fig. 1d, e).

Lidocaine-Reduced IBA1$^+$ Microglia and Suppressed Neuroinflammation

To evaluate the effect of lidocaine on the accumulation of microglia, we used immunological staining of IBA1 to determine the presentation of microglia in the spinal cord at the termination of the behavioral tests. Compared to rats in the sham group, those in the CCI group showed significantly higher staining of IBA1 (23.59 ± 4.32 vs. 8.61 ± 2.36%, $p < 0.05$). We also observed that lidocaine injection significantly decreased the IBA1$^+$ microglia to 12.65 ± 3.12% in spinal cord of CCI rats ($p < 0.05$) (Fig. 2a, b). Similarly, lidocaine injection greatly decreased expression of inflammatory cytokines IL-6 and IL-1β in CCI rats, as measured by RT-PCR (Fig. 2c, d). To promote microglia activation, BV-2 microglia were cultivated with LPS in vitro. Lidocaine pre-treatment significantly reduced expression of IBA1 in LPS-stimulated BV-2 cells (Fig. 2e, f). Moreover, lidocaine

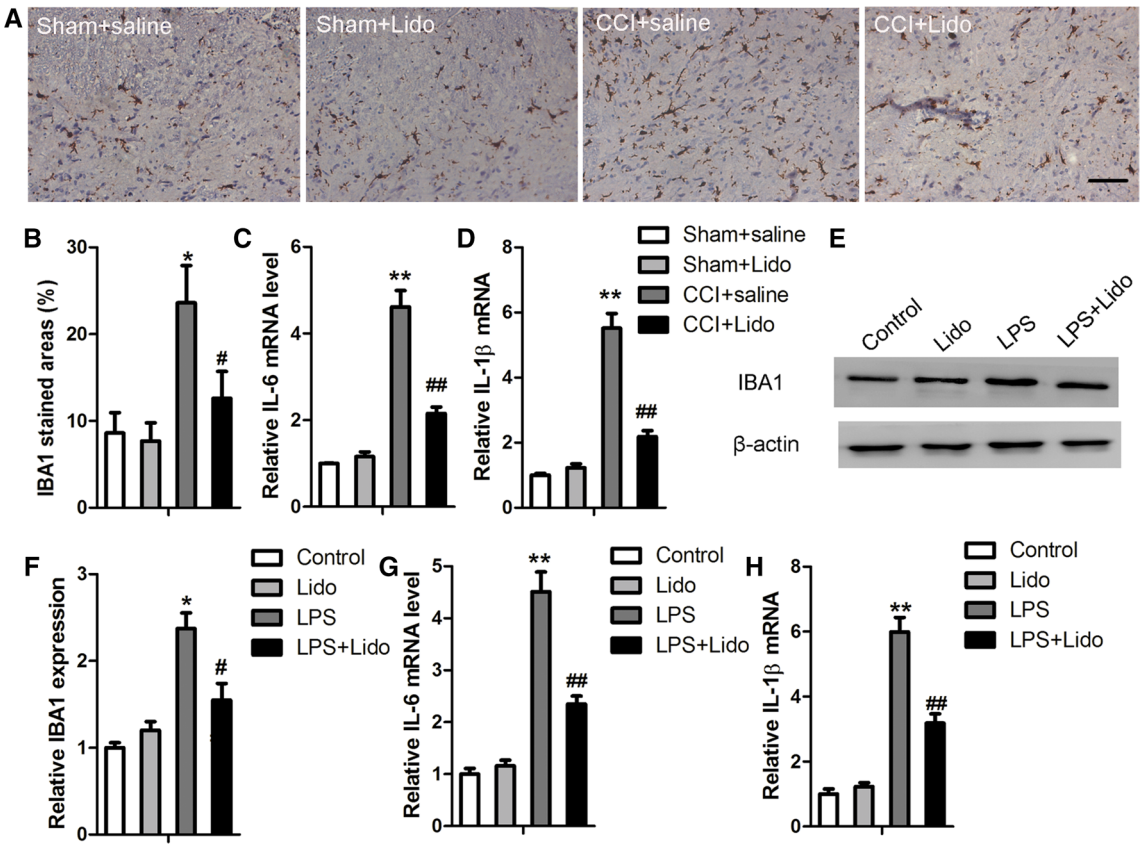

Fig. 2 Inhibitory effect of lidocaine on microglia in CCI rats and LPS-stimulated BV-2 cells. **a** Representative immunohistochemical staining of hyperactive microglia using IBA1 antibody in spinal dorsal horn of CCI or sham rats 14 days postoperatively, scale bar: 100 μm; **b** Quantitative analysis of IBA1 antibody stained areas in spinal section in these animals; **c**, **d** IL-6 and IL-1β mRNA levels in spinal dorsal horn of CCI or sham rats receiving lidocaine or saline. $N = 6$ rats/group, $^*p < 0.05$, $^{**}p < 0.01$ versus Sham + saline; $^{\#}p < 0.05$, $^{\#\#}p < 0.01$ versus CCI + saline. $N = 6$ rats/group; **e**, **f** BV-2 cell were preconditioned with 10 μg/mL of lidocaine for 1 h and then exposed to 1.0 μg/mL LPS for 24 h. Western blot detection and quantification of IBA1 expression in BV-2 cells were performed to evaluate the effect of lidocaine. **g**, **h** L-6 and IL-1β mRNA levels in BV-2 cells. $^*p < 0.05$, $^{**}p < 0.01$ versus Control; $^{\#}p < 0.05$, $^{\#\#}p < 0.01$ versus LPS

also suppressed IL-6 and IL-1β secretion in LPS-stimulated BV-2 cells (Fig. 2g, h).

Lidocaine Upregulated SOCS3 in a pCREB-Dependent Manner in Microglia

SOCS3 helps to control cytokine signaling to eliminate severe systemic inflammation. We aimed to investigate whether SOCS3 was a potential target of lidocaine in suppressing microglia. The SOCS3-expressing cells and IBA1 positive cells in spinal cord were co-localized in the four groups of rats. It was found that 7.08 ± 2.15% of $SOCS3^+$ $IBA1^+$ co-localized cells relative to total $IBA1^+$ cells presented in the spinal cords of rats in the sham group that received a saline injection. While in sham rats receiving lidocaine injection, the ratio of the co-localized cells did not substantially change in comparison with the control group. The ratio of $SOCS3^+$ $IBA1^+$ cells notably decreased to 4.12 ± 2.01% in rats of the CCI group that received saline. However, the co-localized cells were greatly enriched and reached 16.38 ± 4.01% in rats in the CCI group that received lidocaine (Fig. 3a, b).

In addition, in the in vitro study, lidocaine effectively elevated the expression of SOCS3 in BV-2 cells. Meanwhile, SOCS3 expression significantly decreased in BV-2 cells in response to the LPS treatment, while it was rescued after lidocaine incubation. We then investigated whether lidocaine-increased SOCS3 was CREB-dependent and found that p-CREB was expressed in a similar pattern as lidocaine-increased SOCS3 while no significant change to the total CREB in response to lidocaine pretreatment. CREB siRNA was transfected into BV-2 cells to inhibit its expression, and the induction effect of lidocaine on SOCS3 significantly dropped after CREB suppression (Fig. 3c, d).

SOCS3 Influenced Pain and Microglia Accounts Induced by Chronic Constriction Injury

To confirm whether SOCS3 was involved in CCI-evoked pain and microglia accumulation, SOCS3 lentivirus vectors (LV-SOCS3) or its control vectors (LV-Ctrl) were intrathecally injected into the spinal cords of the animals 3 days before CCI injury. After 3 days of recovery, the animals then underwent CCI surgery. SOCS3 mRNA expression

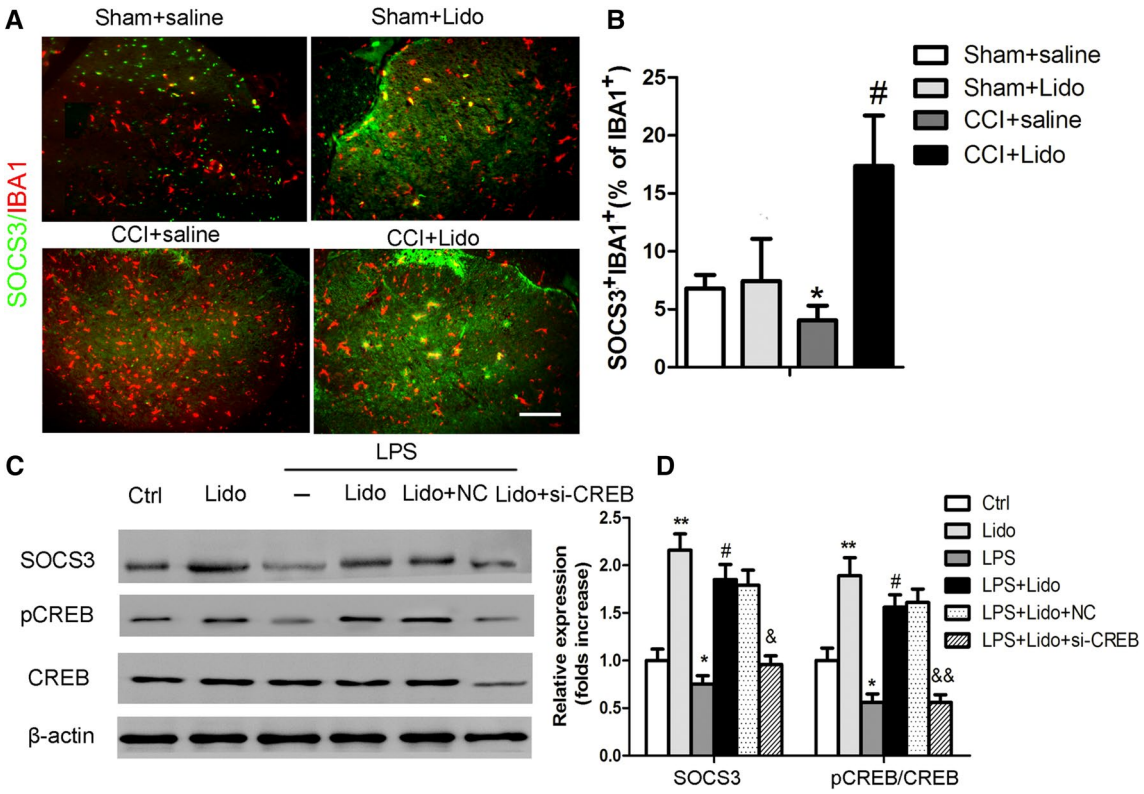

Fig. 3 Lidocaine potentiated the expression of SOCS3 in microglia of CCI rats and activated BV-2 cells in a CREB-dependent manner. **a** Double immunofluorescence staining of the co-localization of SOCS3 expressing cells with $IBA1^+$ microglia in response to CCI and lidocaine exposure. Scale bar: 200 μm $N = 6$ rats/group; $^*p < 0.05$ versus Sham + saline; $^{\#}p < 0.05$ versus CCI + saline; **b** Quantification of the ratio of $SOCS3^+IBA1^+$ cells relative to $IBA1^+$ microglia in each group of animals; **c**, **d** Western blot analysis and quantification of the effects of lidocaine treatment on CREB phosphorylation and SOCS3 expression as well as the regulatory effect of CREB on SOCS3. $^*p < 0.05$, $^{**}p < 0.01$, versus control; $^{\#}p < 0.05$ versus LPS; $^{\&}p < 0.05$, $^{\&\&}p < 0.01$ versus LPS + Lido + NC

was adequately promoted in the spinal cords 2 days after CCI (Fig. 4a). Meanwhile, we detected the transfection efficiency of LV-SOCS3 into the spinal microglia using double labeling of SOCS3 and IBA1 in CCI animals. It was shown that 41.25 ± 14.65% of IBA1$^+$ glial cells expressed SOCS3 in the spinal cord of LV-SOCS3 injected rats, which was significantly higher than that in the LV-Ctrl infected rats (4.6 ± 3.5%) ($p < 0.01$) (Fig. 4b, c). During the behavioral tests, rats injected with LV-SOCS3 showed higher mechanical withdrawal thresholds and thermal withdraw latencies than those injected with LV-Ctrl (Fig. 4d). We also found that LV-SOCS3 notably decreased IBA1$^+$ microglia cells, as shown by the attenuated staining of IBA1 (25.64 ± 4.33%) in comparison with its matched control (8.22 ± 3.56%) ($p < 0.05$) (Fig. 4e, f). In LPS-activated BV-2 cells, SOCS3 transfection profoundly inhibited the expression of IBA1 (Fig. 4g).

Lidocaine-Upregulated SOCS3 Suppressed Inflammation by Inhibiting NF-κB and p38-MAPK

To further explore the function and mechanism of Lido-SOCS3 in suppressing neuroinflammation, BV-2 cells were cultivated in response to lidocaine treatment and SOCS3

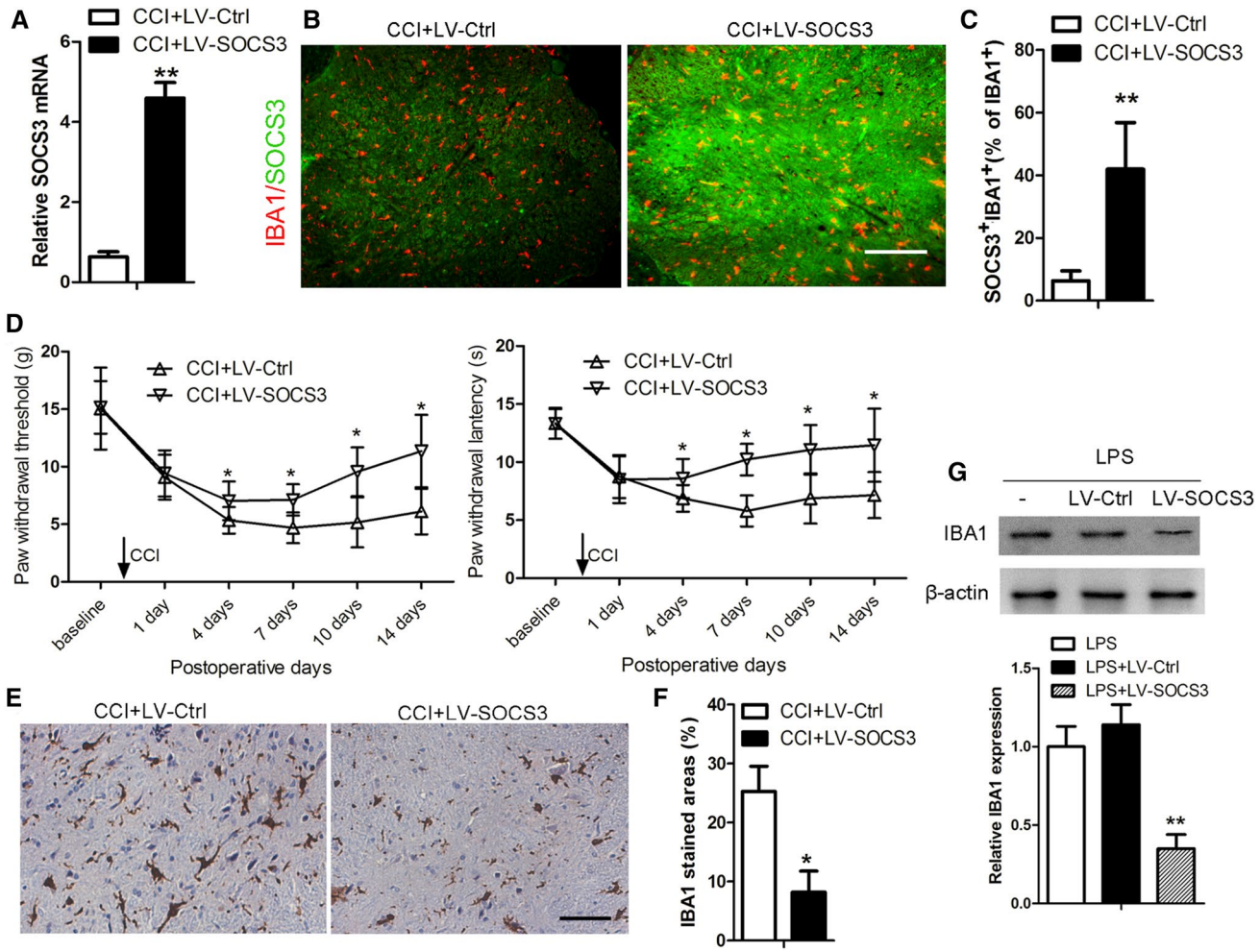

Fig. 4 SOCS3 overexpression alleviated neuropathic pain in CCI rats and microglia activation. CCI animals were intrathecally injected with LV-SOCS3 or LV-Ctrl vectors 3 days prior to the CCI, then behavioral tests and histological examinations were performed after the injections. **a** Evaluation of spinal SOCS3 mRNA levels in rats 48 h after the injection. **b** Double immunofluorescence staining of SOCS3$^+$ with IBA1$^+$ microglia to examine the transfection efficiency of SOCS3 to microglia in CCI rats; Scale bar: 200 μm **c** Quantification of the ratio of SOCS3$^+$IBA1$^+$ cells relative to IBA1$^+$ microglia in each group of animals, $N = 6$ rats/group; **d** The effects of SOCS3 overexpression on mechanical allodynia (paw withdrawal thresholds) and thermal hyperalgesia (paw withdrawal lantency) of CCI rats. $N = 6$ rats/group. **e**, **f** Effect of SOCS3 overexpression on the presentation of IBA1$^+$ spinal microglia in CCI rats. Scale bar: 100 μm; $N = 6$ rats/group. The differences between groups were analyzed by t test or repeated ANOVA followed by LSD tests. *$p < 0.05$, **$p < 0.01$ versus CCI + LV-Ctrl. **g** BV-2 cells were transfected with SOCS3 overexpressing vectors or control for 48 h and incubated with LPS for another 24 h, then the IBA1 expression was determined using western blot. **$p < 0.01$ versus LPS + LV-Ctrl

vector transfection and the inflammatory mediators were determined. It was shown that LPS dramatically boosted the production of IL-6 from baseline level of 30.2 ± 4.6 pg/mL to 220.7 ± 25.3 pg/mL, IL-1β from 8.1 ± 1.5 pg/mL to 25.6 ± 4.1 pg/mL and TNF-α from 181.3 ± 21.4 to 682.6 ± 45.8 pg/mL in BV-2 cells (each $p < 0.01$). IL-6 decreased to 138.2 ± 18.6 pg/mL and 85.7 ± 15.5 pg/mL after lidocaine treatment and SOCS3 overexpression, respectively (each $p < 0.05$). Mean time, IL-1β and TNF-α were also extensively decreased in response to lidocaine treatment and SOCS3 overexpression. The inhibitory effects on the secretion of these inflammatory mediators were further potentiated by concurrent lidocaine treatment and SOCS3 upregulation (Fig. 5a–c). Besides, LPS increased phosphorylated p65 and p38 by approximately 1.1 and 1.7 folds compared to their control levels (each $p < 0.01$). The relative expressions of LPS-stimulated p-p65 and p-p38 reduced about 26% and 32% after lidocaine treatment, and about 46% and 48% after SOCS3 overexpression (each $p < 0.05$). The combination of lidocaine and SOCS3 had a further inhibitory effect on the expressions of phosphorylated p65 and p38 (Fig. 5d).

Discussion

Lidocaine is a local anesthetic that is frequently used in clinical practice for its anti-arrhythmic and nerve conduction-blocking effects. Lidocaine acts on voltage-gated sodium channels to alleviate neuropathic pain and to attenuate chronic analgesic tolerance. However, the underlying mechanisms of lidocaine in suppressing neuropathic pain are unclear. Our study demonstrated that lidocaine could upregulate SOCS3 to suppress microglia and inflammation, which in turn alleviating neuropathic pain.

Nerve injury can be caused by surgery, trauma, burns, and other injuries. During nerve injury, peripheral nociceptors are evoked. These nociceptors are involved in the transition from acute pain to chronic pain. The impulse conduction from the peripheral lesion potentiates the responses of pain circuits in the spinal cord and brain, which causes pain to spread (Ji et al. 2016). In addition to neurons, other cells (immune, glia, and stem cells) in the peripheral and central nervous systems also play critical roles in the initiation, maintenance, and resolution of pain. Microglial cells are important CNS components that function as resident macrophages in the spinal cord and brain. Microglia rapidly activate and proliferate when signal inputs from peripheral nerve

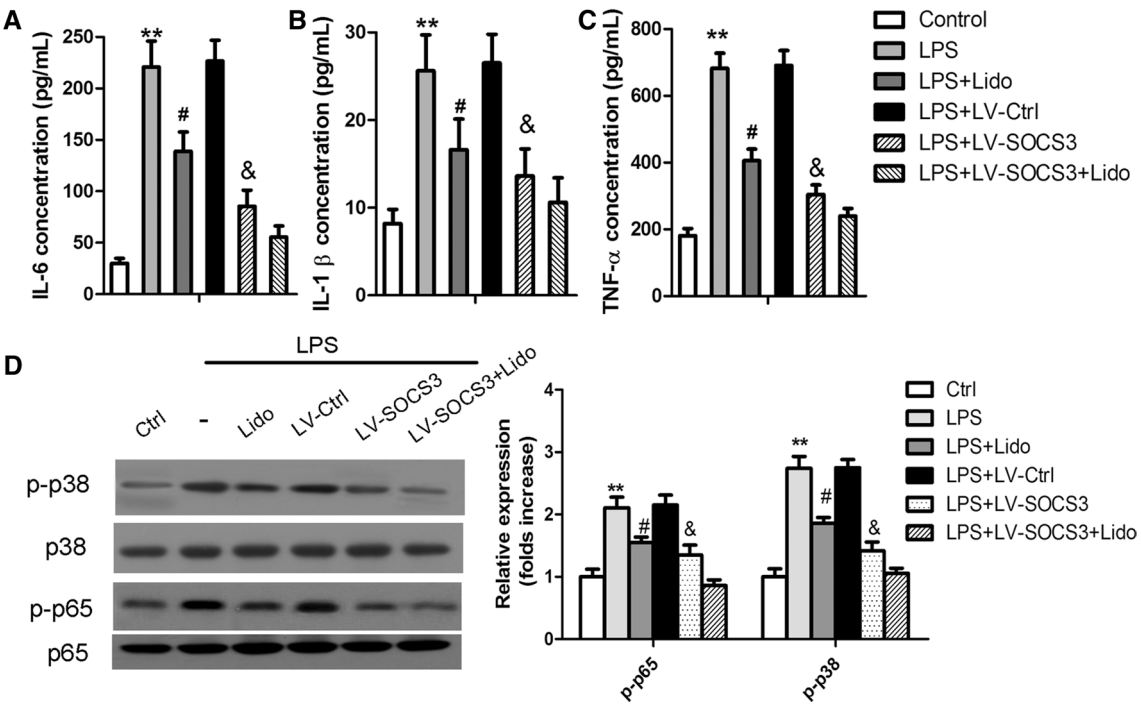

Fig. 5 SOCS3 overexpression suppressed neuroinflammation by inhibiting NF-κB and p38-MAPK signaling in BV-2 cells. BV-2 cells were transfected with SOCS3 overexpressing vectors or the matched control vectors, and were pretreated using lidocaine followed by the addition of LPS. **a–c** After 24 h of incubation, supernatant IL-1β, IL-6 and TNF-α levels in each culture were evaluated by ELISA. **d** Activation of NF-κB and p38-MAPK signaling cascades in BV-2 cells in response to various treatments were determined by western blot. $^{**}p < 0.01$ versus Control; $^{\#}p < 0.05$ versus LPS; $^{\&}p < 0.05$ versus LPS + LV-Ctrl

injury or pathological changes in the CNS are perceived. In the current study, we also found that the number of $IBA1^+$ microglia increased in the dorsal horn of spinal cord after CCI surgery.

Recent researches have focused on the effects of lidocaine on glia and neuroinflammation. Localized neuroinflammation that occurs in response to trauma or injury of the peripheral and central nervous systems contributes to neuropathic pain. Activated microglia are main sources of inflammatory mediators. We observed that intrathecally injected lidocaine attenuated CCI-induced neuropathic pain and suppressed spinal microglia proliferation and inflammatory mediators production, all of which may contribute to its analgesic effects. Cheng et al. have reported that intrathecal lidocaine pretreatment retarded acute spinal nerve ligation (SNI)-induced neuropathic pain for 3 days by inhibiting Nav1.3 expression and spinal microglia activation (Cheng et al. 2011). Lidocaine also can alleviate diabetes-induced tactile allodynia by inhibiting microglial activation (Suzuki et al. 2011). Lidocaine significantly inhibits the release and expression of nitric oxide, MCP 1, prostaglandin E2, IL-1β, and TNF-α in LPS-activated microglia (Yuan et al. 2014).

SOCS3 participates in multiple diseases, such as bacterial and viral infections, cancer, and diabetes (Mahony et al. 2016). Its roles in nervous diseases remain unclear. SOCS3 was reported to function in neuronal protection and axon regeneration after spinal cord injury (Liu et al. 2015). It also suppressed the transition of microglia to the M1 phenotype by blocking IL-6 in Aβ-challenged primary microglia, indicating its involvement in Alzheimer's disease (Iwahara et al. 2017). In our study, we noticed that SOCS3 was normally expressed in spinal microglia and was downregulated in $IBA1^+$ microglia that were exposed to peripheral injury. Its restoration by lidocaine alleviated neuropathic pain in rats that underwent CCI surgery.

We found that lidocaine modulated SOCS3 expression in a pCREB-depending manner. The transcription factor CREB plays important roles in the regulation of hyperalgesia and in the orchestration of synaptic plasticity and chronic pain development by modulating pain-related gene expression (Hu et al. 2017). CREB is activated by phosphorylation at serine133 (pCREB), after which it can dimerize and translocate to nucleus to stimulate the transcription of downstream target genes (Yu et al. 2017). Currently, mechanisms by which the SOCS3 gene is regulated are poorly revealed. Chakrabarti et al. have reported that cinnamic acid upregulates the expression of SOCS3 in glial cells via CREB pathway, which potentially suppresses neuroinflammation in the pathogenesis of various neurodegenerative diseases. It is predicted by the Genomatix Software that the cAMP response element (CRE) sequence between 1534 and 1555 base are positioned upstream of the SOCS3 open reading frame. Therefore, the author has proposed that activated CREB could be recruited to CRE sequence to initiate the transcription of *SOCS3* (Chakrabarti et al. 2018). Besides, Kim et al. also found that CREB-modulated cytokine signaling in part by upregulating SOCS3 in stromal cells and they identified SOCS3 as a cAMP-regulated CREB target gene (Kim et al. 2017). Therefore, the phosphorylated CREB functions to enhance the SOCS3 expression at least in part by its recruitment to the CRE sequence locating in the promoter of *SOCS3*. With regard to the induction of lidocaine on the phosphorylation of CREB, we considered that lidocaine might affect the activities of PKA, PKC and cAMP and so on, which functioned to modulate the activation of CREB. It was confirmed that lidocaine was positively correlated with cAMP accumulation in gingival fibroblasts (Villarruel et al. 2011). In addition, study by Zhang et al. revealed that lidocaine-enhanced adenosine 5′-monophosphate (AMP)-activated protein kinase (AMPK) phosphorylation in a calcium-dependent protein kinase kinase β (CaMKKβ)-dependent manner (Zhang et al. 2017). However, more understanding about the mechanism of lidocaine in modulating pCREB-SOCS3 pathway should be replenished and updated in further studies. SOCS3 overexpression in the dorsal root ganglion attenuated mechanical allodynia associated with bone cancer (Wei et al. 2017). Compelling research highlighted the role of SOCS3 induction on postoperative pain by inhibiting neuroinflammation (Fan et al. 2018). Cianciulli and Boontanrart's studies have confirmed that chemical compounds like folic acid and vitamin D3 can elevate SOCS3, which in turn increasing expression of anti-inflammatory mediators in BV-2 microglia (Boontanrart et al. 2016; Cianciulli et al. 2016). We confirmed that SOCS3 overexpression in BV-2 cells protected against inflammation by suppressing p38-MAPK and NF-κB. SOCS family members can degrade specific cytokine receptors to control cytokine action, which may represent another potential anti-inflammatory mechanism of SOCS3, which should be investigated in future studies (Babon et al. 2014). Zhang et al. have confirmed that lidocaine induces SOCS3 to alleviate morphine tolerance in mice, depending on its role in neuroinflammation suppression (Zhang et al. 2017). Our study confirmed the inductive role of lidocaine on SOCS3 in the spinal cords of rats that were exposed to CCI insult.

Collectively, our study demonstrated that intrathecal injection of lidocaine could alleviate mechanical and thermal pain caused by CCI surgery. Lidocaine induced SOCS3 expression in a CREB-dependent manner in microglia, which then suppressed p38-MAPK and NF-κB to control neuroinflammation. Our findings may represent a new understanding on how lidocaine alleviates pain and thus may help to identify optional treatments for patients with peripheral chronic pain.

Author Contributions YZ and SBY conceived and designed the study; YZ drafted the manuscript and conducted the experiments. XHH analyzed and interpreted the data; SBY critically revised the manuscript; All authors have read and approved the final manuscript.

Compliance with Ethical Standards

Conflict of interest The authors declare that they have no conflict of interest.

Ethical Approval All procedures performed in studies involving animals were in accordance with the ethical standards of the institution or practice at Jilin University.

References

Babon JJ, Varghese LN, Nicola NA (2014) Inhibition of IL-6 family cytokines by SOCS3. Semin Immunol 26:13–19. https://doi.org/10.1016/j.smim.2013.12.004

Becker DE, Reed KL (2012) Local anesthetics: review of pharmacological considerations. Anesth Prog 59:90–101. https://doi.org/10.2344/0003-3006-59.2.90 **quiz 102–103**

Berta T, Lee JE, Park CK (2017) Unconventional role of caspase-6 in spinal microglia activation and chronic pain. Mediators Inflamm 2017:9383184. https://doi.org/10.1155/2017/9383184

Boontanrart M, Hall SD, Spanier JA, Hayes CE, Olson JK (2016) Vitamin D3 alters microglia immune activation by an IL-10 dependent SOCS3 mechanism. J Neuroimmunol 292:126–136. https://doi.org/10.1016/j.jneuroim.2016.01.015

Chakrabarti S, Jana M, Roy A, Pahan K (2018) Upregulation of suppressor of cytokine signaling 3 in microglia by cinnamic acid. Curr Alzheimer Res 15:894–904. https://doi.org/10.2174/1567205015666180507104755

Cheng KI, Lai CS, Wang FY, Wang HC, Chang LL, Ho ST, Tsai HP, Kwan AL (2011) Intrathecal lidocaine pretreatment attenuates immediate neuropathic pain by modulating Nav1.3 expression and decreasing spinal microglial activation. BMC Neurol 11:71. https://doi.org/10.1186/1471-2377-11-71

Cianciulli A, Salvatore R, Porro C, Trotta T, Panaro MA (2016) Folic acid is able to polarize the inflammatory response in LPS activated microglia by regulating multiple signaling pathways. Mediators Inflamm 2016:5240127. https://doi.org/10.1155/2016/5240127

Cohen SP, Mao J (2014) Neuropathic pain: mechanisms and their clinical implications. BMJ 348:f7656. https://doi.org/10.1136/bmj.f7656

Costigan M, Scholz J, Woolf CJ (2009) Neuropathic pain: a maladaptive response of the nervous system to damage. Annu Rev Neurosci 32:1–32. https://doi.org/10.1146/annurev.neuro.051508.135531

Eberhardt M, Stueber T, de la Roche J, Herzog C, Leffler A, Reeh PW, Kistner K (2017) TRPA1 and TRPV1 are required for lidocaine-evoked calcium influx and neuropeptide release but not cytotoxicity in mouse sensory neurons. PLoS ONE 12:e0188008. https://doi.org/10.1371/journal.pone.0188008

Fan YX, Qian C, Liu B, Wang C, Liu H, Pan X, Teng P, Hu L, Zhang G, Han Y, Yang M, Wu XF, Liu WT (2018) Induction of suppressor of cytokine signaling 3 via HSF-1-HSP70-TLR4 axis attenuates neuroinflammation and ameliorates postoperative pain. Brain Behav Immun 68:111–122. https://doi.org/10.1016/j.bbi.2017.10.006

Finnerup NB, Attal N, Haroutounian S, McNicol E, Baron R, Dworkin RH, Gilron I, Haanpaa M, Hansson P, Jensen TS, Kamerman PR, Lund K, Moore A, Raja SN, Rice AS, Rowbotham M, Sena E, Siddall P, Smith BH, Wallace M (2015) Pharmacotherapy for neuropathic pain in adults: a systematic review and meta-analysis. Lancet Neurol 14:162–173. https://doi.org/10.1016/S1474-4422(14)70251-0

Gierthmuhlen J, Baron R (2016) Neuropathic pain. Semin Neurol 36:462–468. https://doi.org/10.1055/s-0036-1584950

Gray A, Marrero-Berrios I, Weinberg J, Manchikalapati D, Schianodi-Cola J, Schloss RS, Yarmush J (2016) The effect of local anesthetic on pro-inflammatory macrophage modulation by mesenchymal stromal cells. Int Immunopharmacol 33:48–54. https://doi.org/10.1016/j.intimp.2016.01.019

Hu XM, Zhang H, Xu H, Zhang HL, Chen LP, Cui WQ, Yang W, Shen W (2017) Chemokine receptor CXCR15 regulates CaMKII/CREB pathway in spinal neurons that underlies cancer-induced bone pain. Sci Rep 7:4005. https://doi.org/10.1038/s41598-017-04198-3

Iwahara N, Hisahara S, Kawamata J, Matsumura A, Yokokawa K, Saito T, Fujikura M, Manabe T, Suzuki H, Matsushita T, Suzuki S, Shimohama S (2017) Role of suppressor of cytokine signaling 3 (SOCS3) in altering activated microglia phenotype in APPswe/PS1dE9 mice. J Alzheimers Dis 55:1235–1247. https://doi.org/10.3233/JAD-160887

Jensen TS, Finnerup NB (2014) Allodynia and hyperalgesia in neuropathic pain: clinical manifestations and mechanisms. Lancet Neurol 13:924–935. https://doi.org/10.1016/S1474-4422(14)70102-4

Ji RR, Chamessian A, Zhang YQ (2016) Pain regulation by non-neuronal cells and inflammation. Science 354:572–577. https://doi.org/10.1126/science.aaf8924

Kim JH, Hedrick S, Tsai WW, Wiater E, Le Lay J, Kaestner KH, Leblanc M, Loar A, Montminy M (2017) CREB coactivators CRTC2 and CRTC3 modulate bone marrow hematopoiesis. Proc Natl Acad Sci USA 114:11739–11744. https://doi.org/10.1073/pnas.1712616114

Kuchalik J, Magnuson A, Tina E, Gupta A (2017) Does local infiltration analgesia reduce peri-operative inflammation following total hip arthroplasty? A randomized, double-blind study. BMC Anesthesiol 17:63. https://doi.org/10.1186/s12871-017-0354-y

Kwon M, Han J, Kim UJ, Cha M, Um SW, Bai SJ, Hong SK, Lee BH (2017) Inhibition of mammalian target of rapamycin (mTOR) signaling in the insular cortex alleviates neuropathic pain after peripheral nerve injury. Front Mol Neurosci 10:79. https://doi.org/10.3389/fnmol.2017.00079

Leffler A, Lattrell A, Kronewald S, Niedermirtl F, Nau C (2011) Activation of TRPA1 by membrane permeable local anesthetics. Mol Pain 7:62. https://doi.org/10.1186/1744-8069-7-62

Li TF, Fan H, Wang YX (2015) Epidural sustained release ropivacaine prolongs anti-allodynia and anti-hyperalgesia in developing and established neuropathic pain. PLoS ONE 10:e0117321. https://doi.org/10.1371/journal.pone.0117321

Liang Y, Xu WD, Peng H, Pan HF, Ye DQ (2014) SOCS signaling in autoimmune diseases: molecular mechanisms and therapeutic implications. Eur J Immunol 44:1265–1275. https://doi.org/10.1002/eji.201344369

Liu X, Williams PR, He Z (2015) SOCS3: a common target for neuronal protection and axon regeneration after spinal cord injury. Exp Neurol 263:364–367. https://doi.org/10.1016/j.expneurol.2014.10.024

Mahony R, Ahmed S, Diskin C, Stevenson NJ (2016) SOCS3 revisited: a broad regulator of disease, now ready for therapeutic use? Cell Mol Life Sci 73:3323–3336. https://doi.org/10.1007/s00018-016-2234-x

Matsuura T, Mori T, Hasaka M, Kuno M, Kawawaki J, Nishikawa K, Narahashi T, Sawada M, Asada A (2012) Inhibition of

voltage-gated proton channels by local anaesthetics in GMI-R1 rat microglia. J Physiol 590:827–844. https://doi.org/10.1113/jphysiol.2011.218149

Ohno-Urabe S, Aoki H, Nishihara M, Furusho A, Hirakata S, Nishida N, Ito S, Hayashi M, Yasukawa H, Imaizumi T, Akashi H, Tanaka H, Fukumoto Y (2018) Role of macrophage Socs3 in the pathogenesis of aortic dissection. J Am Heart Assoc 7(2):e007389. https://doi.org/10.1161/JAHA.117.007389

Suzuki N, Hasegawa-Moriyama M, Takahashi Y, Kamikubo Y, Sakurai T, Inada E (2011) Lidocaine attenuates the development of diabetic-induced tactile allodynia by inhibiting microglial activation. Anesth Analg 113:941–946. https://doi.org/10.1213/ANE.0b013e31822827a2

Toda S, Sakai A, Ikeda Y, Sakamoto A, Suzuki H (2011) A local anesthetic, ropivacaine, suppresses activated microglia via a nerve growth factor-dependent mechanism and astrocytes via a nerve growth factor-independent mechanism in neuropathic pain. Mol Pain 7:2. https://doi.org/10.1186/1744-8069-7-2

Villarruel EQ, Borda E, Sterin-Borda L, Orman B (2011) Lidocaine-induced apoptosis of gingival fibroblasts: participation of cAMP and PKC activity. Cell Biol Int 35:783–788. https://doi.org/10.1042/CBI20100200

Wang Z, Huang H, Yang S, Huang S, Guo J, Tang Q, Qi F (2016) Long-term effect of ropivacaine nanoparticles for sciatic nerve block on postoperative pain in rats. Int J Nanomed 11:2081–2090. https://doi.org/10.2147/IJN.S101563

Wei J, Li M, Wang D, Zhu H, Kong X, Wang S, Zhou YL, Ju Z, Xu GY, Jiang GQ (2017) Overexpression of suppressor of cytokine signaling 3 in dorsal root ganglion attenuates cancer-induced pain in rats. Mol Pain 13:1744806916688901. https://doi.org/10.1177/1744806916688901

Yin Y, Liu W, Dai Y (2015) SOCS3 and its role in associated diseases. Hum Immunol 76:775–780. https://doi.org/10.1016/j.humimm.2015.09.037

Yu XW, Oh MM, Disterhoft JF (2017) CREB, cellular excitability, and cognition: implications for aging. Behav Brain Res 322:206–211. https://doi.org/10.1016/j.bbr.2016.07.042

Yuan T, Li Z, Li X, Yu G, Wang N, Yang X (2014) Lidocaine attenuates lipopolysaccharide-induced inflammatory responses in microglia. J Surg Res 192:150–162. https://doi.org/10.1016/j.jss.2014.05.023

Zhang Y, Tao GJ, Hu L, Qu J, Han Y, Zhang G, Qian Y, Jiang CY, Liu WT (2017) Lidocaine alleviates morphine tolerance via AMPK-SOCS3-dependent neuroinflammation suppression in the spinal cord. J Neuroinflamm 14:211. https://doi.org/10.1186/s12974-017-0983-6

Zhuang ZY, Wen YR, Zhang DR, Borsello T, Bonny C, Strichartz GR, Decosterd I, Ji RR (2006) A peptide c-Jun N-terminal kinase (JNK) inhibitor blocks mechanical allodynia after spinal nerve ligation: respective roles of JNK activation in primary sensory neurons and spinal astrocytes for neuropathic pain development and maintenance. J Neurosci 26:3551–3560. https://doi.org/10.1523/JNEUROSCI.5290-05.2006